Lensing statistics around the low-density-positions

Fuyu Dong
Collaborator: Jun Zhang, Yu Yu, Xiaohu Yang, Wentao Luo, et al.
Shanghai Jiao Tong University
ISSI-BJ, 2019/11/07

Outline

1. Motivation & Background

2. Method: low density position(LDP)

3. Data & Results

4. Summary

1. Motivation: Dark Energy

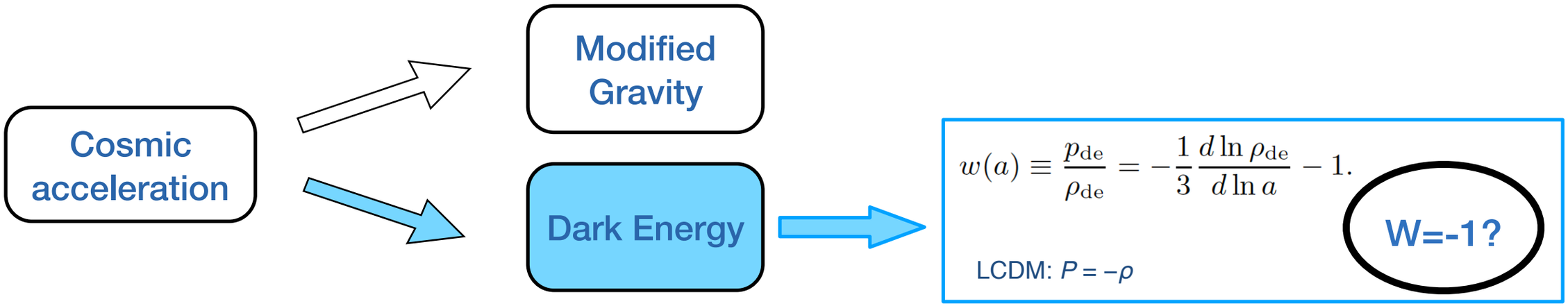

Evidence of existence

- Type Ia Supernovae
- Cosmic microwave background
- Baryon acoustic oscillations (BAO)
- Integrated Sachs–Wolfe effect (ISW)
- Lensing
- ……

Different H(z) and Growth

$$H^2/H_0^2 = \Omega_m a^{-3} + \sum_{i'} \Omega_{i'} e^{3\int_a^1 [1+w_{i'}(a')]da'/a'}$$

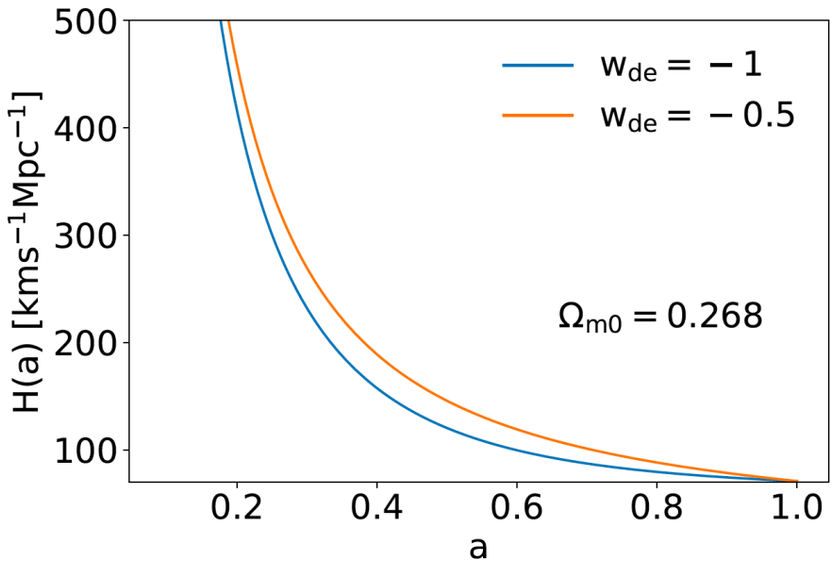

Challenges of the Void Lensing

1. Large Radius -> Limited numbers;
2. Hard to define the void center;
3. Unclear boundaries.

⇨ Low signal-to-noise Ratio

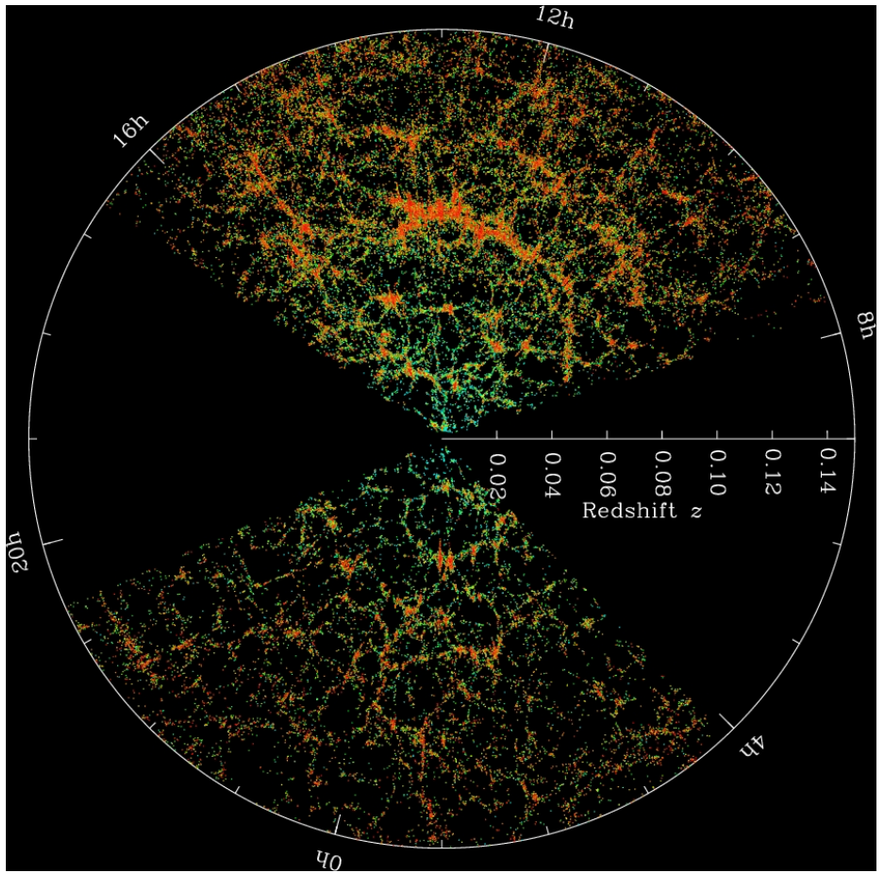

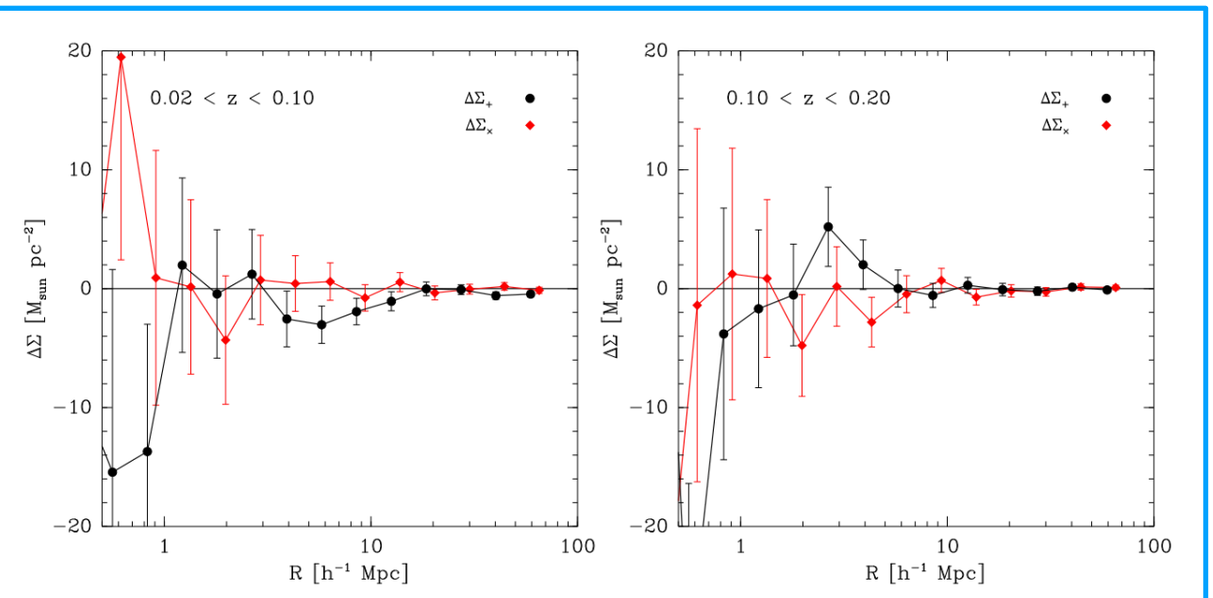

Figure A1. Lensing E-mode ($\Delta\Sigma_+$, *black*) and B-mode ($\Delta\Sigma_\times$, *red*) for voids in two separate redshift bins. The signal was averaged as a function of physical radius rather than in units the void radius.

901 voids, void finder: ZOBOV
SDSS DR7 galaxies

1309.2045

2. The Main Idea: the Low Density Position (LDP)

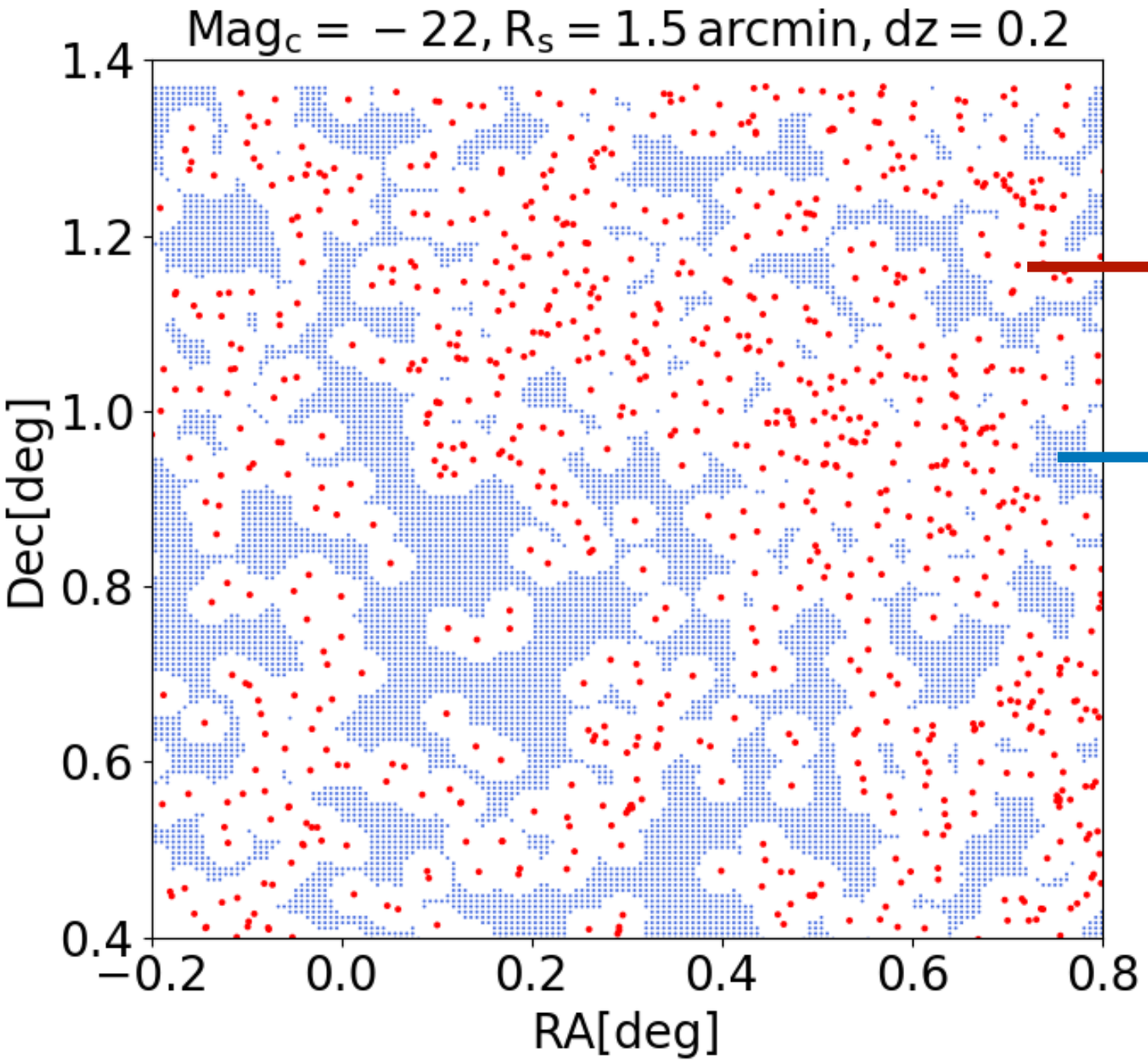

Galaxies that are projected in a z slice

Bright galaxies

LDPs

Advatages:

Do not need accurate z;
Plenty of LDPs;
Without defining centers.

$$z_m = 0.435, Mag_c = -22, R_s = 1.5\ arcmin$$

Test the LDP lensing in observation - CFHTLenS shear catalogue

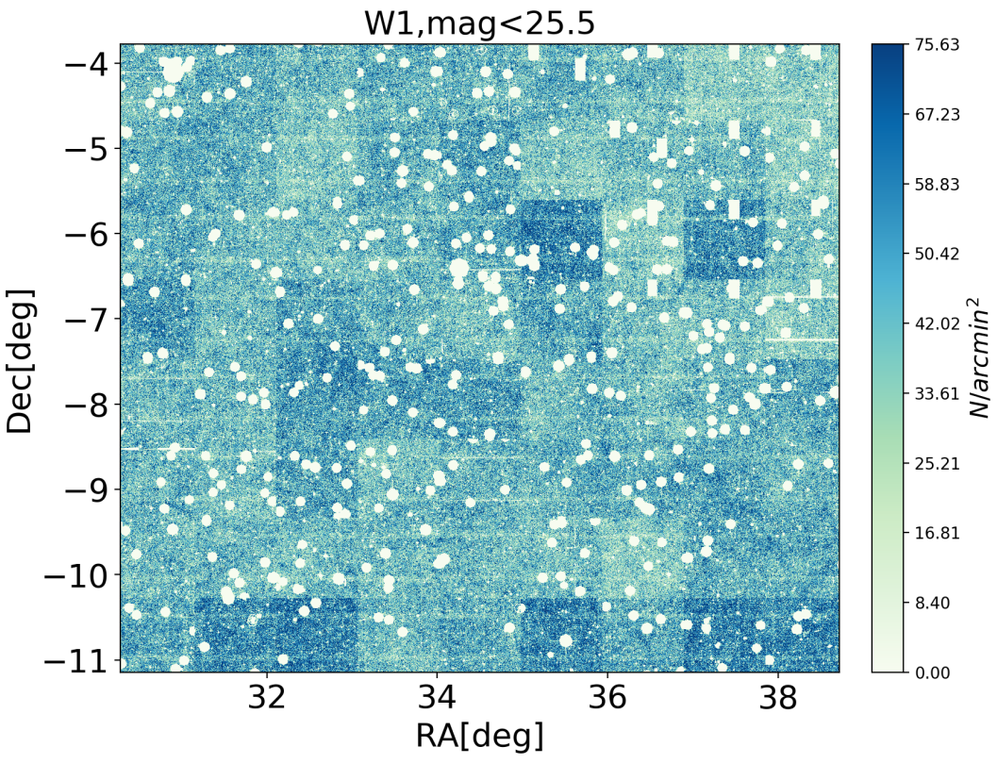

Foreground galaxy selection

1. Star_flag == 0

2. Two or more close height peaks in redshift PDF

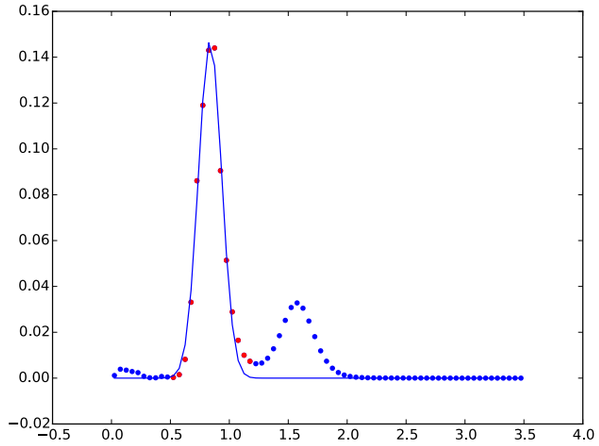

3. Galaxies with Mag_i<-99

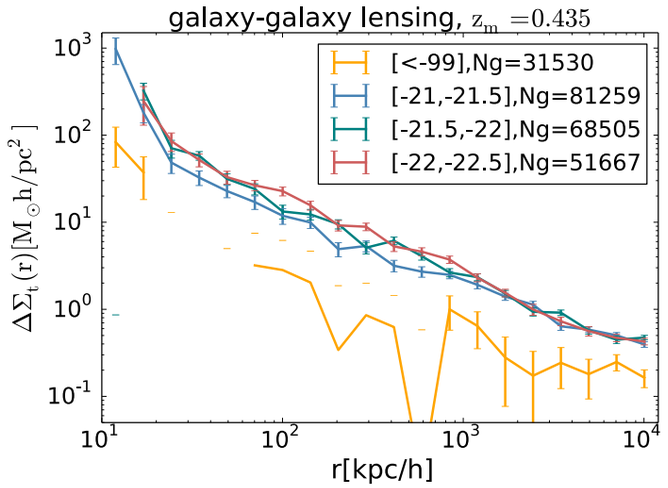

1. It comprise 171 pointings, effective survey area of about 154 deg^2. W1,W2,W3,W4.
2. Shear measurement with Lensfit (Miller et al. 2013)
3. Photometric redshift measurement with the BPZ code (Hildebrandt et al. 2012).

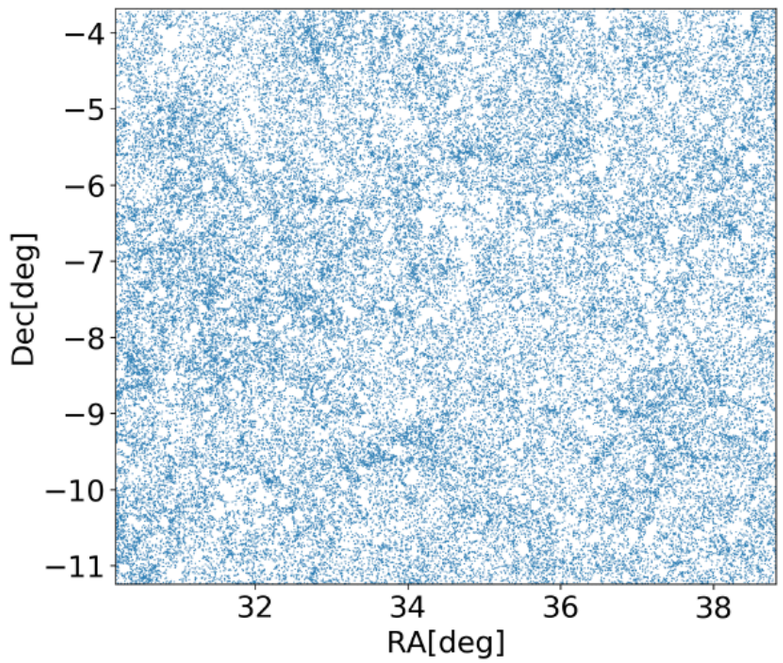

Figure 2. The panel shows galaxy distribution in W1 with absolute magnitude $\mathrm{Mag_i} < -21.5$, $0.335 < z < 0.535$.

the Low-Density-Position (LDP) & the Mask Effect

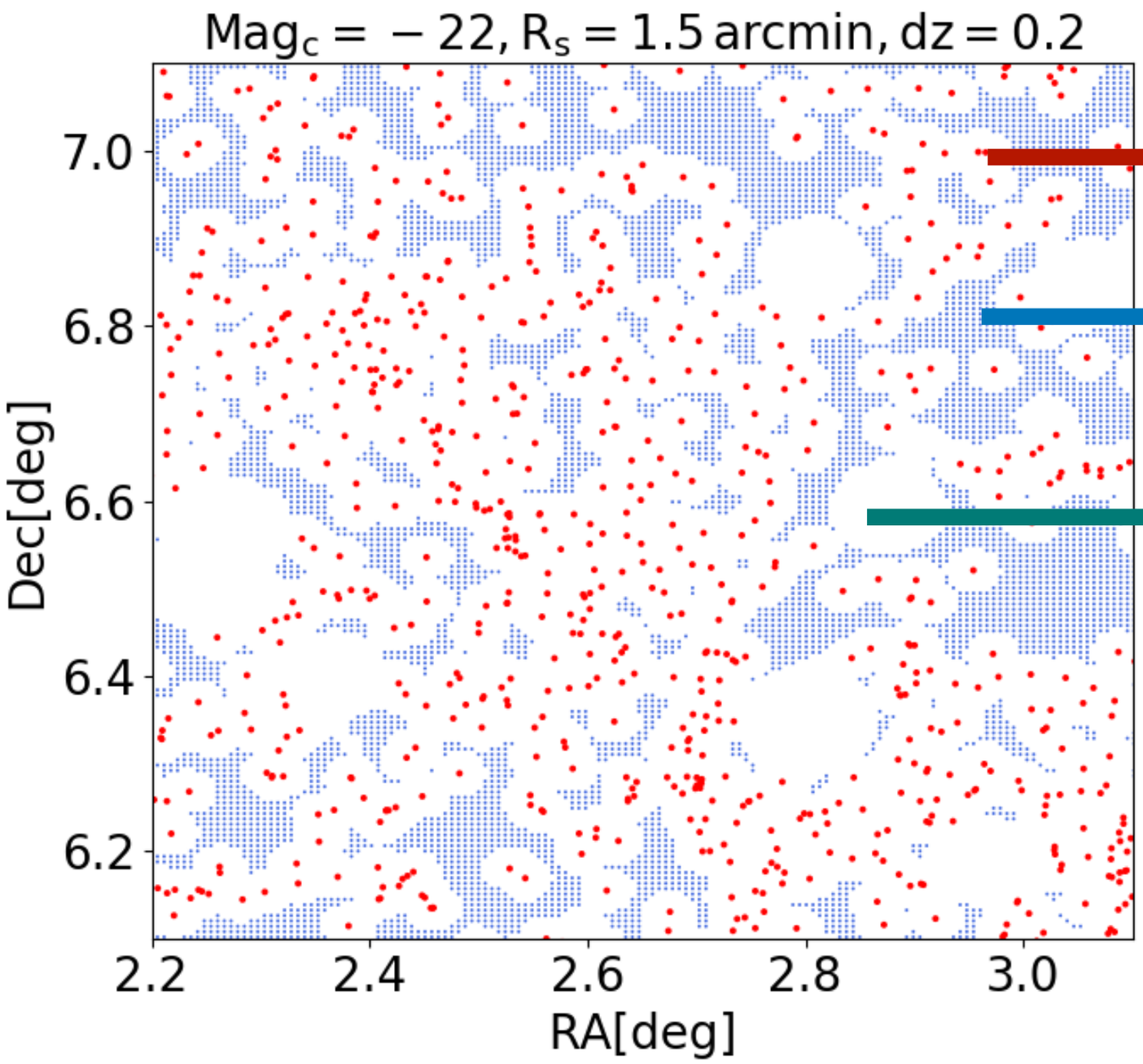

Bright galaxies

LDPs

Masks

Operations with Masks:

$$\frac{S_{mask}}{\pi R_s^2} < 0.1$$

3. Result: 2D LDP-Lensing signals in CFHTLenS

Observation:

Sources

↓

Foreground galaxy sample

↓

Generating LDP candidates

↓

Finding out LDPs

Mask map

↓

Lensing signals

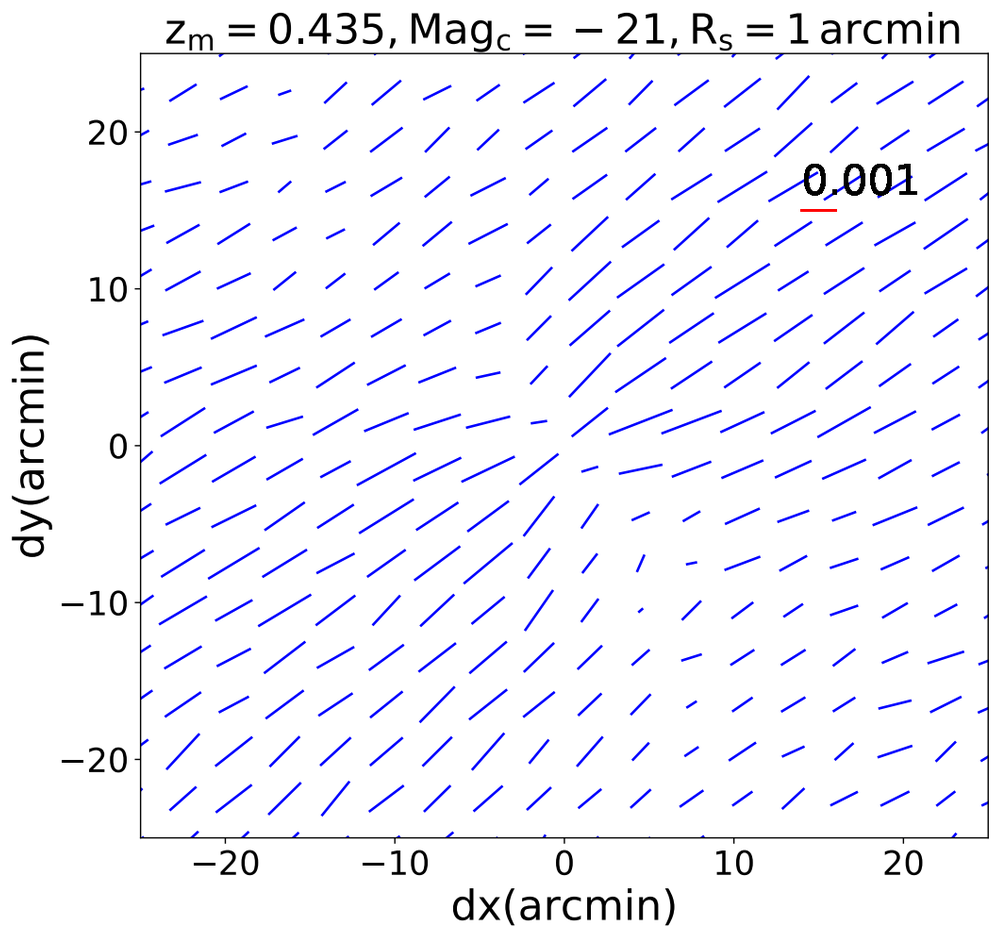

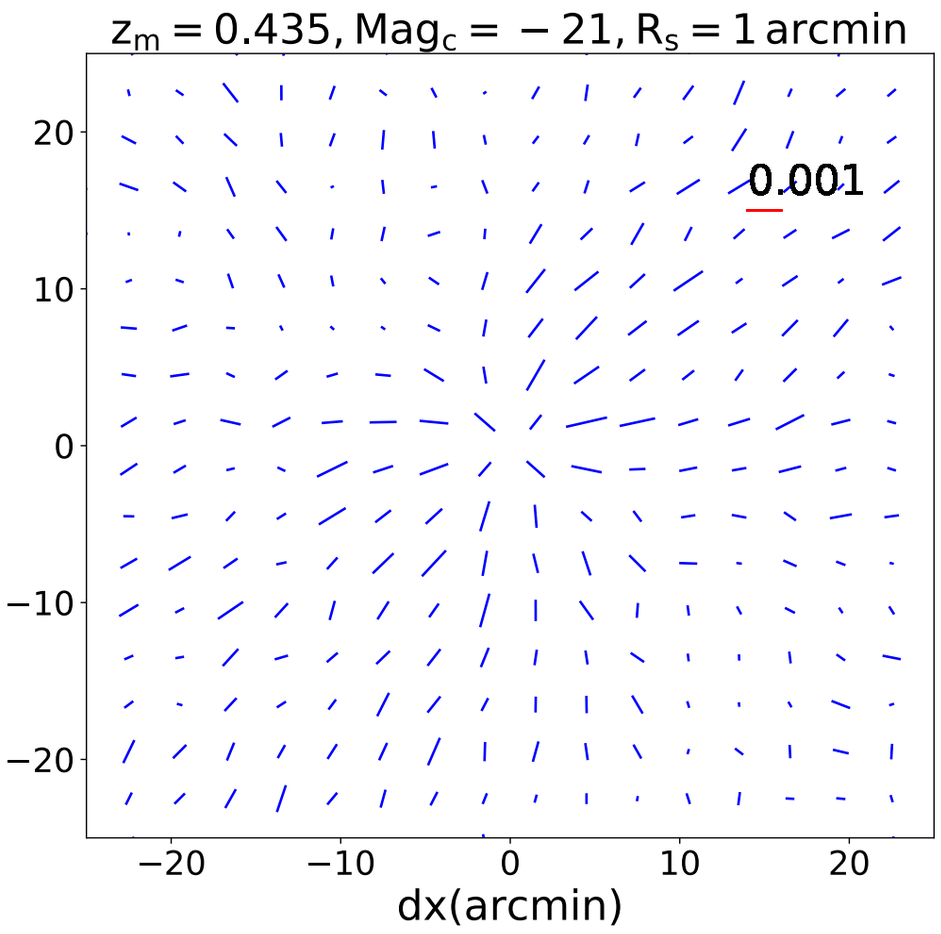

$$\gamma_{1,2} = \frac{\Sigma_i w_i \left(\epsilon_{i(1,2)} - c_{i(1,2)}\right)}{\Sigma_i w_i (1 + m_i)}$$

↓

Concave lens shear patterns

$$\gamma_{1,2} - \overline{\gamma}_{rand,1,2}$$

Simulation - Different w(z)

Table 1. Simulation parameters.

Simulation	w_{de}	σ_8	Ω_c	Ω_b	h	n_s
CW1	-1	0.85	0.223	0.045	0.71	1
CW2	-0.5	(0.633)	0.223	0.045	0.71	1
CW3	-0.8	(0.789)	0.223	0.045	0.71	1
CW4	-1.2	(0.893)	0.223	0.045	0.71	1
Simulation	w_{de}	A_s	Ω_c	Ω_b	h	n_s
WZ1	-1	2.2e-9	0.2568	0.0485	0.679	0.968
WZ2	w(z)	2.2e-9	0.24188	0.04525	0.702	0.966

CAMB: P(k), (Lewis et al. 2000)
2LPT: Initial condition, (Springel & Hernquist 2002)
Gadget2: simulation, (Springel 2005)

i) For CW1, we produce the initial condition following parameters ($\sigma_8 = 0.85, \Omega_c = 0.223$, $\Omega_b = 0.045, n_s = 1$). For CW2,3,4 the same initial conditions are used, with updated H(z) for different w_{de} model in Gadget2. The value of σ_8 in the 4 simulations reduces with increasing w.

ii) For the second set, we adopt the best fit cosmological parameters from Zhao et al. (2017) for ΛCDM and dynamical dark energy w(z) model, and use CAMB (Lewis et al. 2000) to generate the initial power spectrum for the simulation.

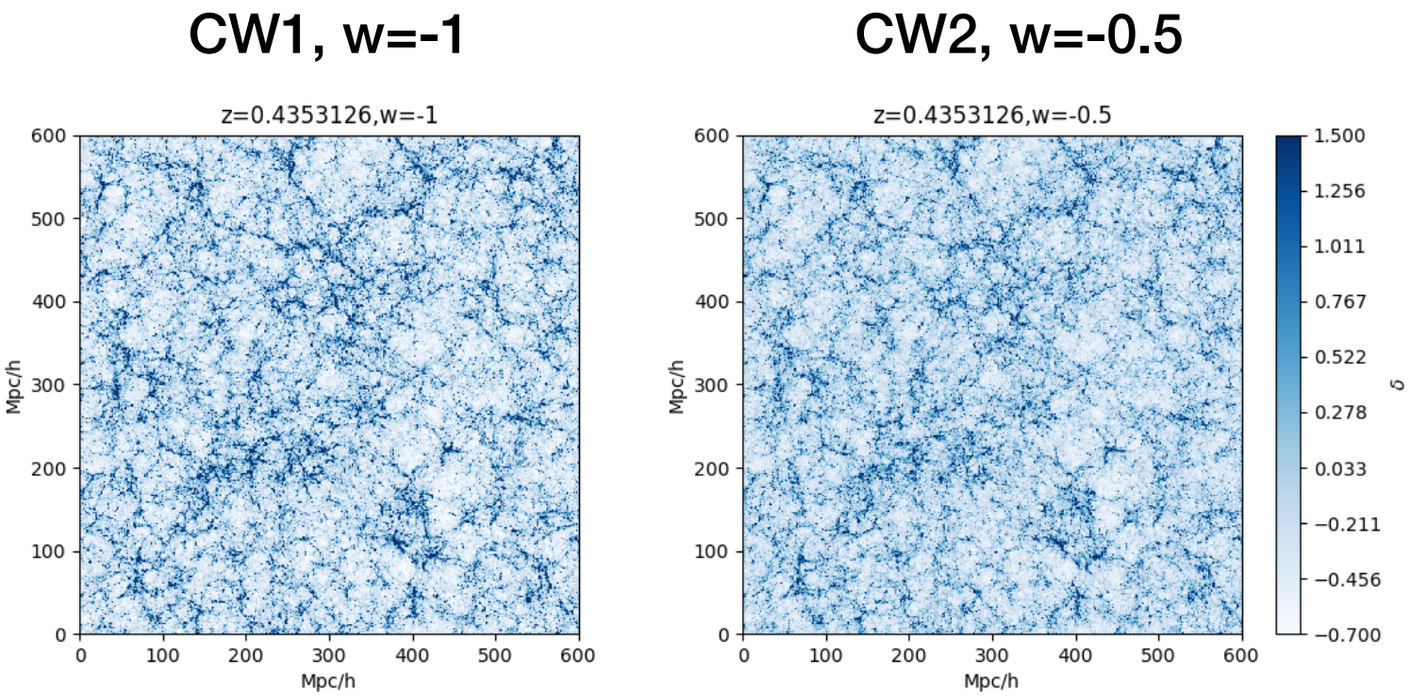

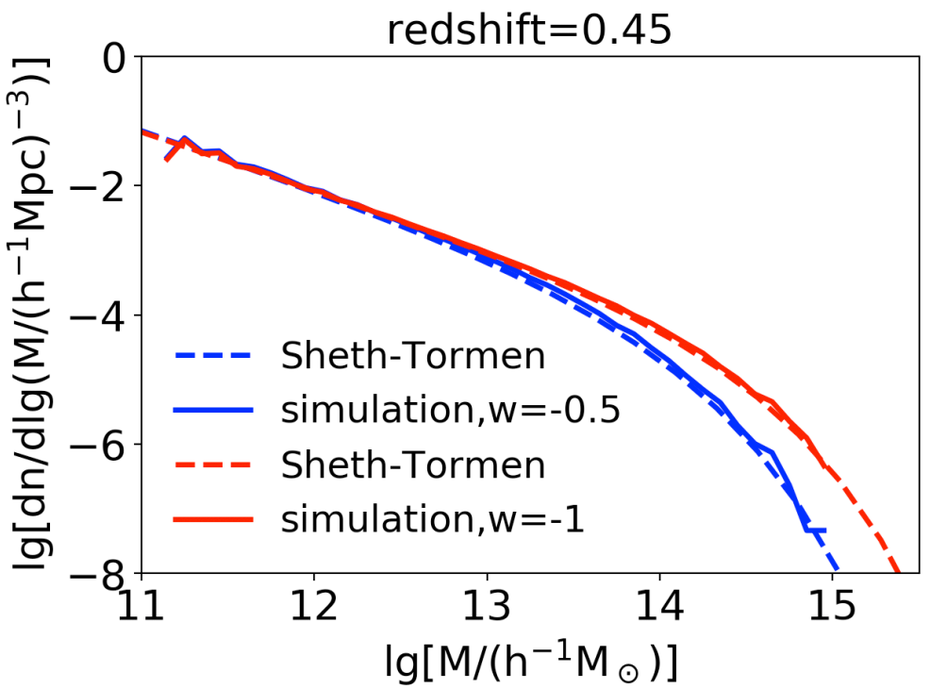

Linking the Galaxy to Subhalo/Halo

subhalo abundance matching(SHAM)

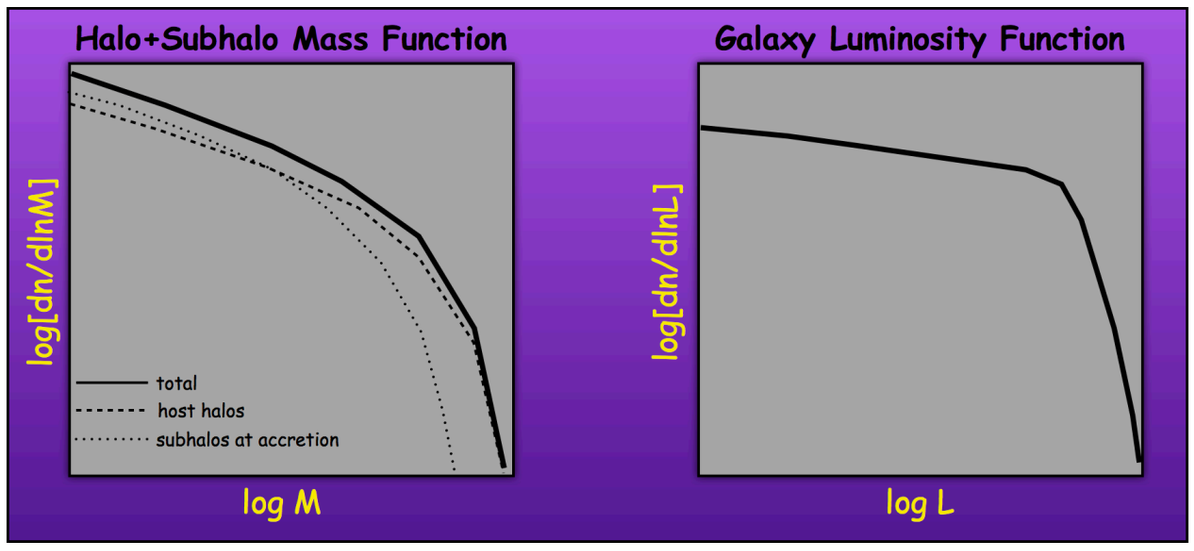

$$\int_L^\infty \phi(L)dL = \int_M^\infty [n_h(M) + n_{sh}(M)]dM$$

SHAM, e.g., Vale & Ostriker 2004

mock galaxy distribution

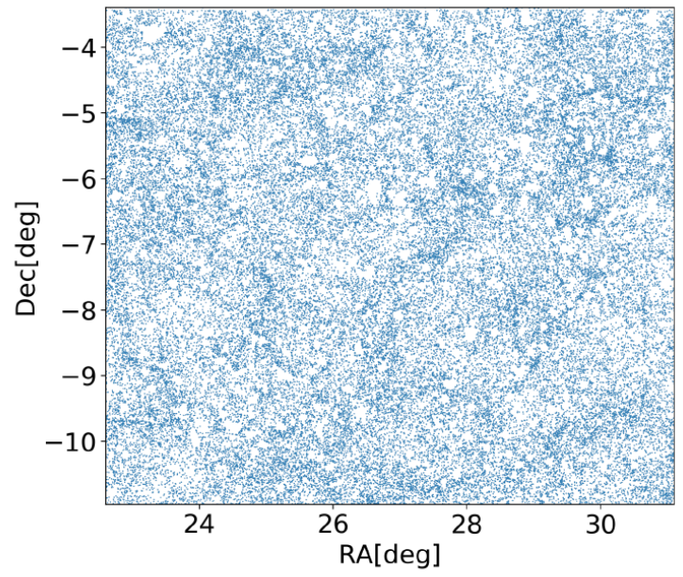

Figure 3. The figure shows galaxy distribution from one sub-area of CW1 simulation for Mag_i <-21.5, $0.335 < z < 0.535$.

HBT: subhalo, (Han et al. 2012)

Surface Density of LDP in Simulation

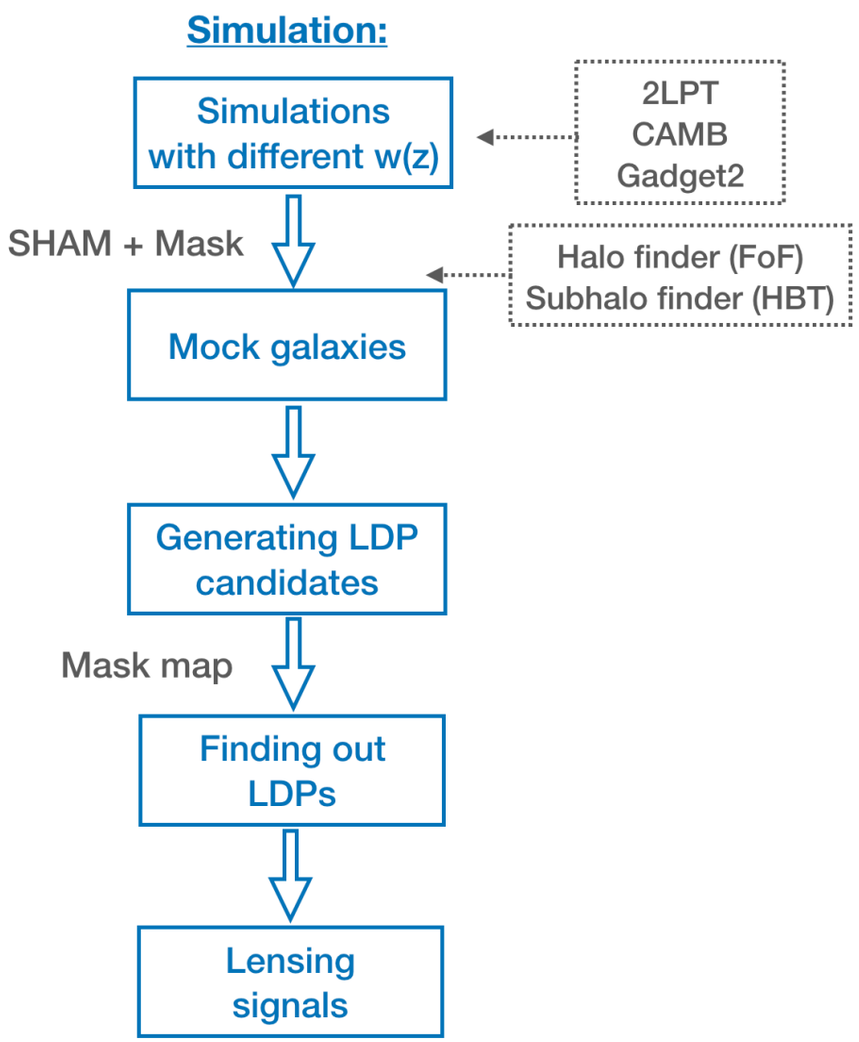

$$\Delta\Sigma(\mathrm{R}) \equiv \Sigma_{\mathrm{cr}}(\mathrm{z_l}, \mathrm{z_s})\langle\gamma_{\mathrm{t}}\rangle(\mathrm{R}) = \overline{\Sigma}(<\mathrm{R}) - \overline{\Sigma}(\mathrm{R})$$

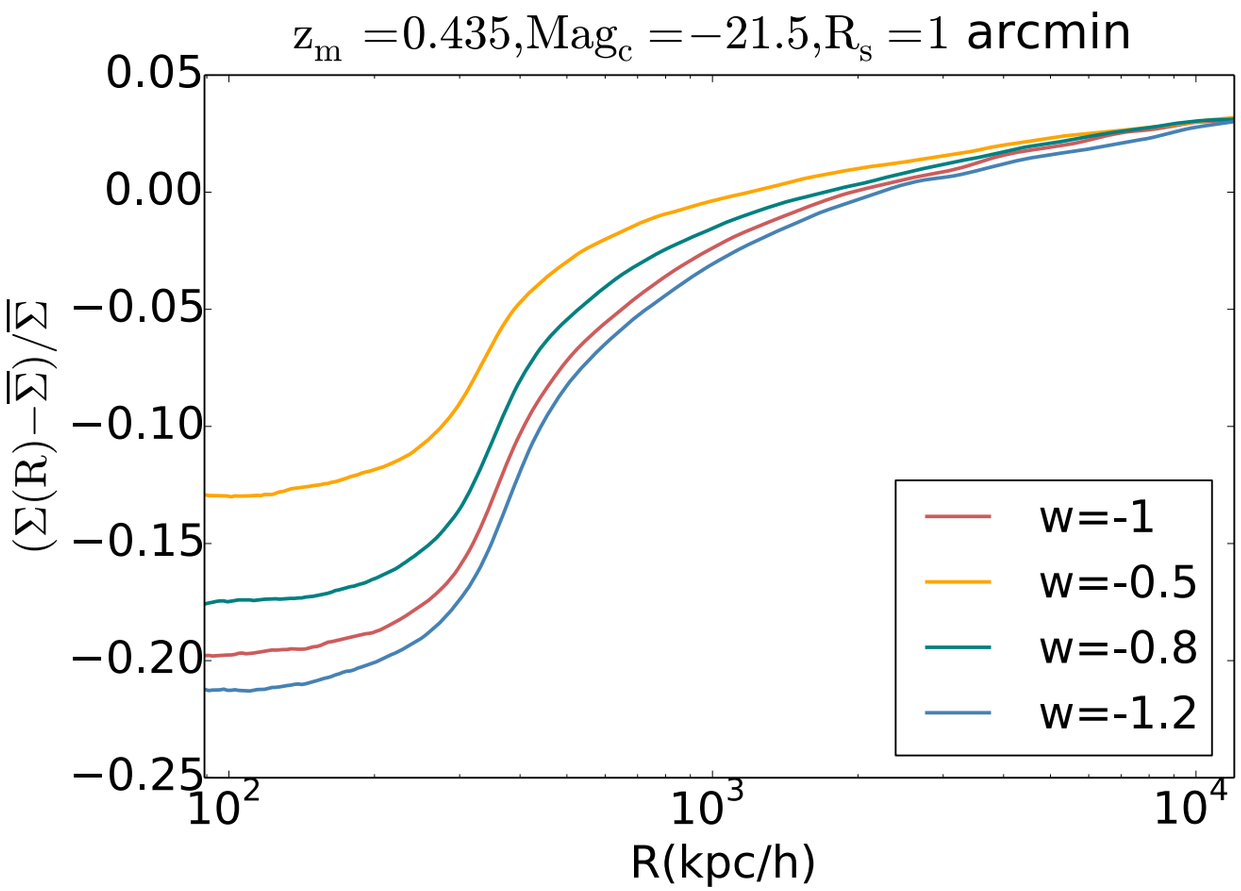

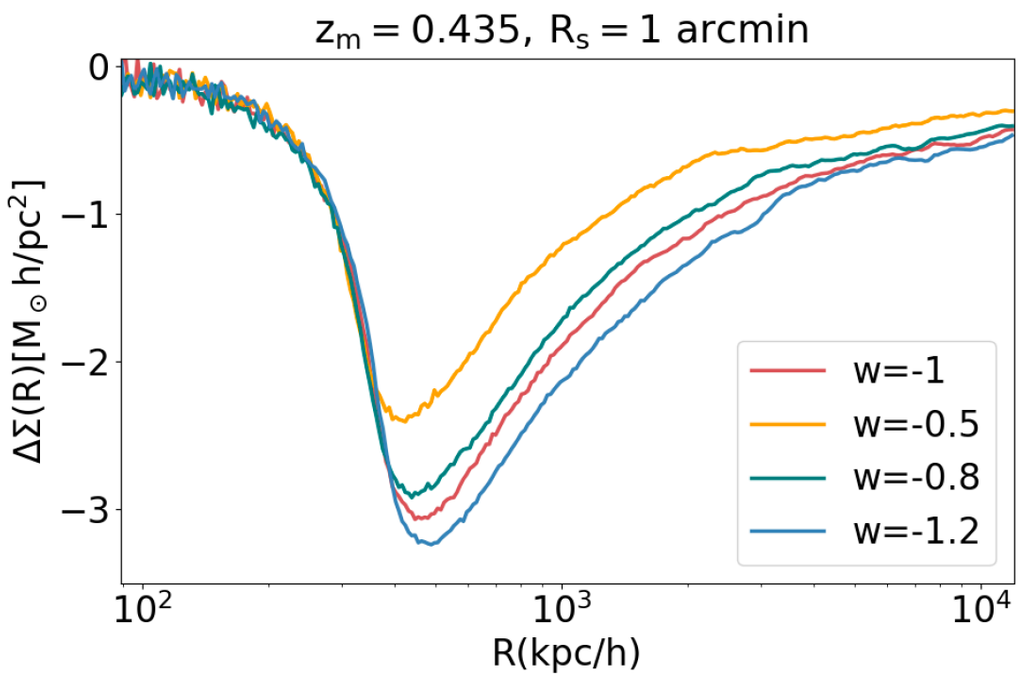

Comparing the observational signal to the simulation signal

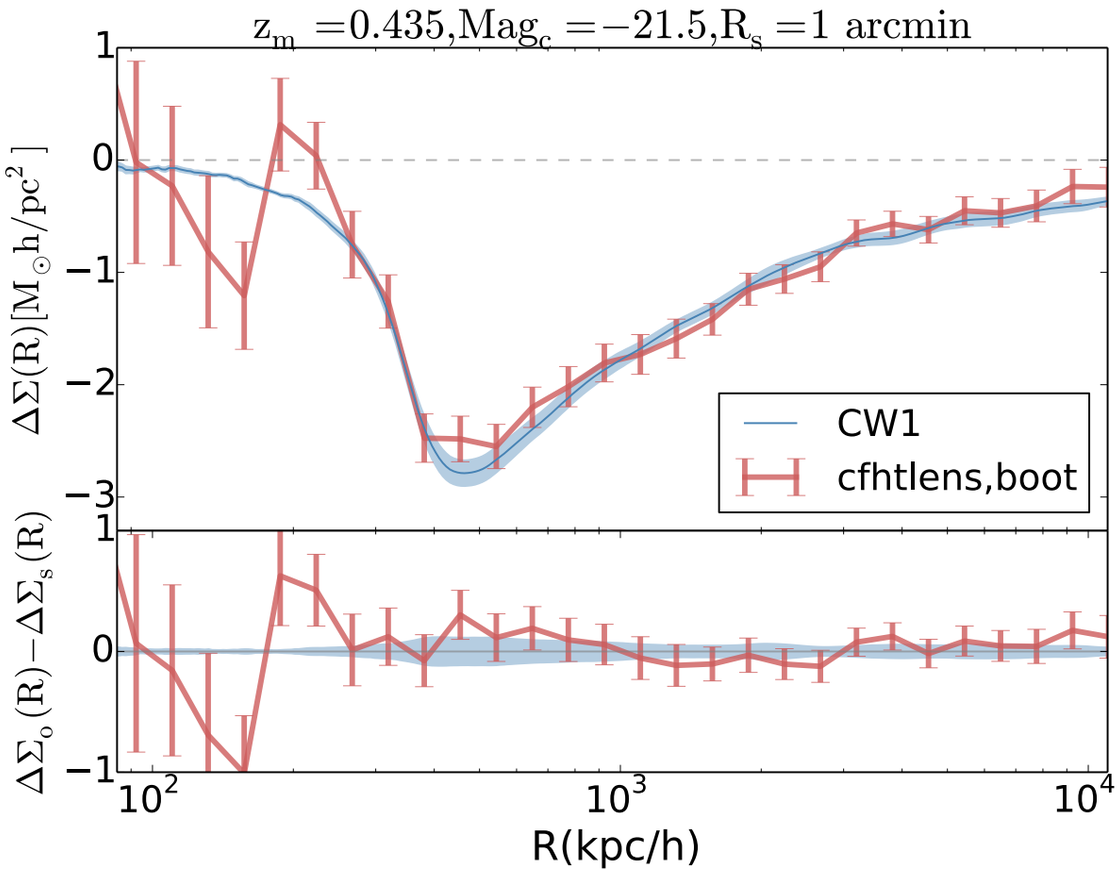

$$\langle \Delta\Sigma \rangle (R) = \frac{1}{N} \sum_{a=1}^{N_c} \sum_{s_a : \left| \lg\left(\frac{R_{s_a}}{R}\right) \right| < \Delta} w(a, s_a) \Sigma_{cr(a)} \epsilon_{(s_a)+}(R_{s_a}), \tag{6}$$

$$N = \sum_{a=1}^{N_c} \sum_{s_a} w(a, s_a) \,. \tag{7}$$

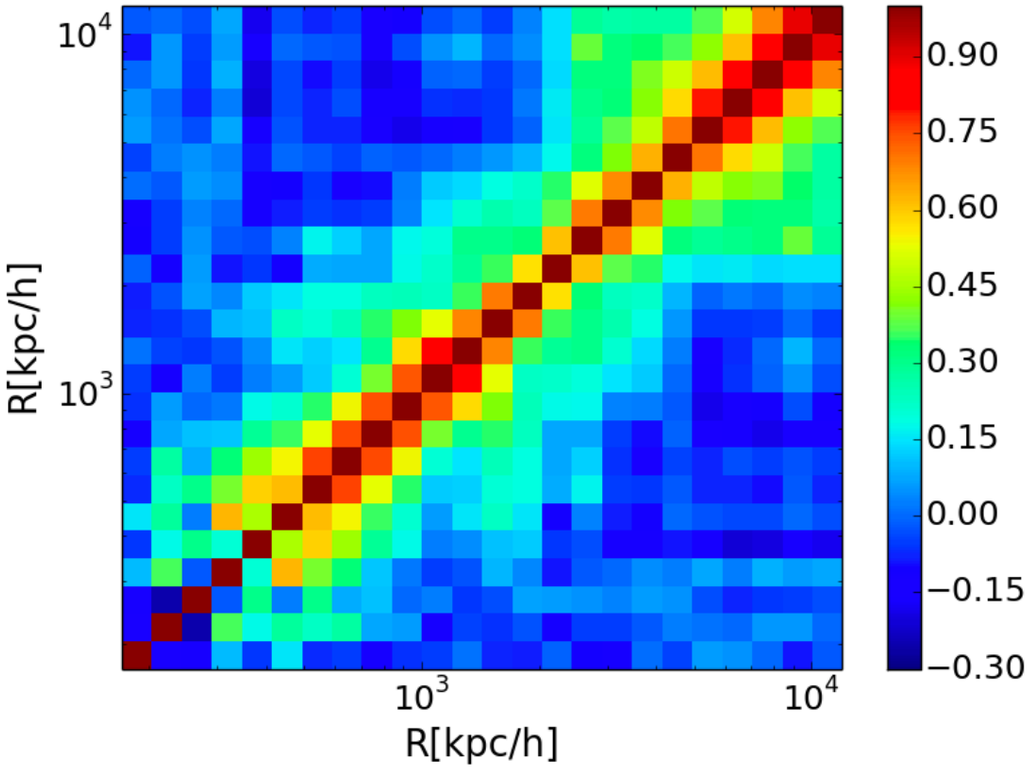

$$\left(\frac{S}{N}\right)^2 = \sum_{i,j} \Delta\Sigma_o(\theta_i) C^{-1}_{i,j} \Delta\Sigma_o(\theta_j),$$

$$C^{-1}_{i,j} = \frac{N_S - N_D - 2}{N_S - 1} C^{*-1}_{i,j},$$

$$C^*_{i,j} = \mathrm{cov}(\Delta\Sigma_o(\theta_i), \Delta\Sigma_o(\theta_j)),$$

S/N = 20.473

All Results

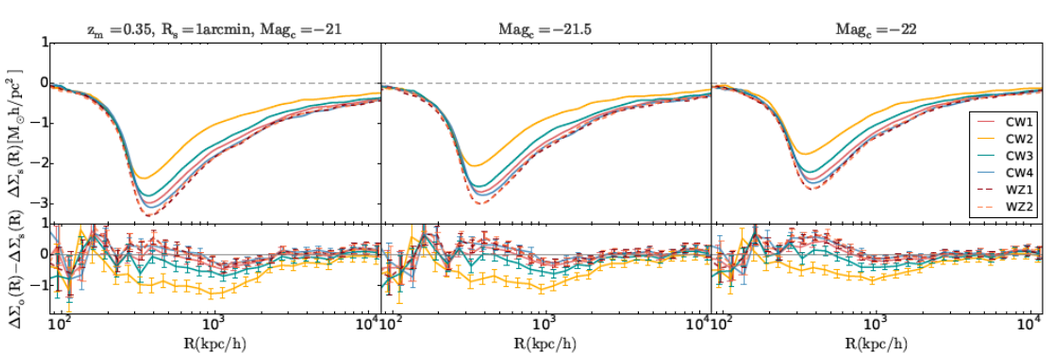

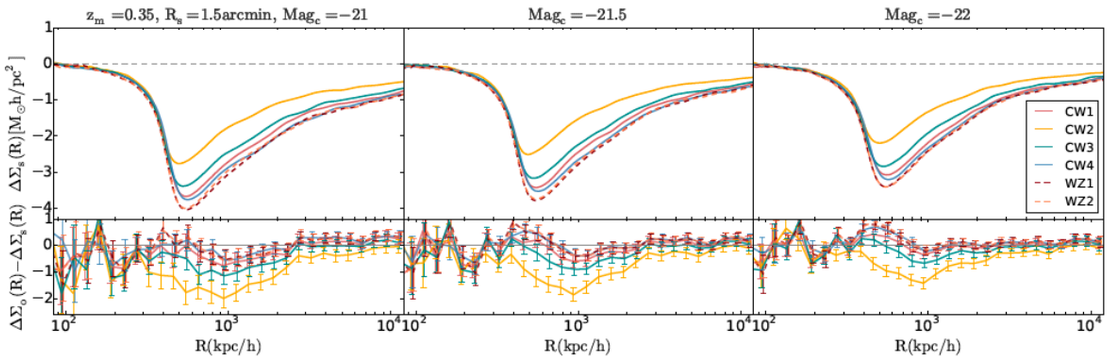

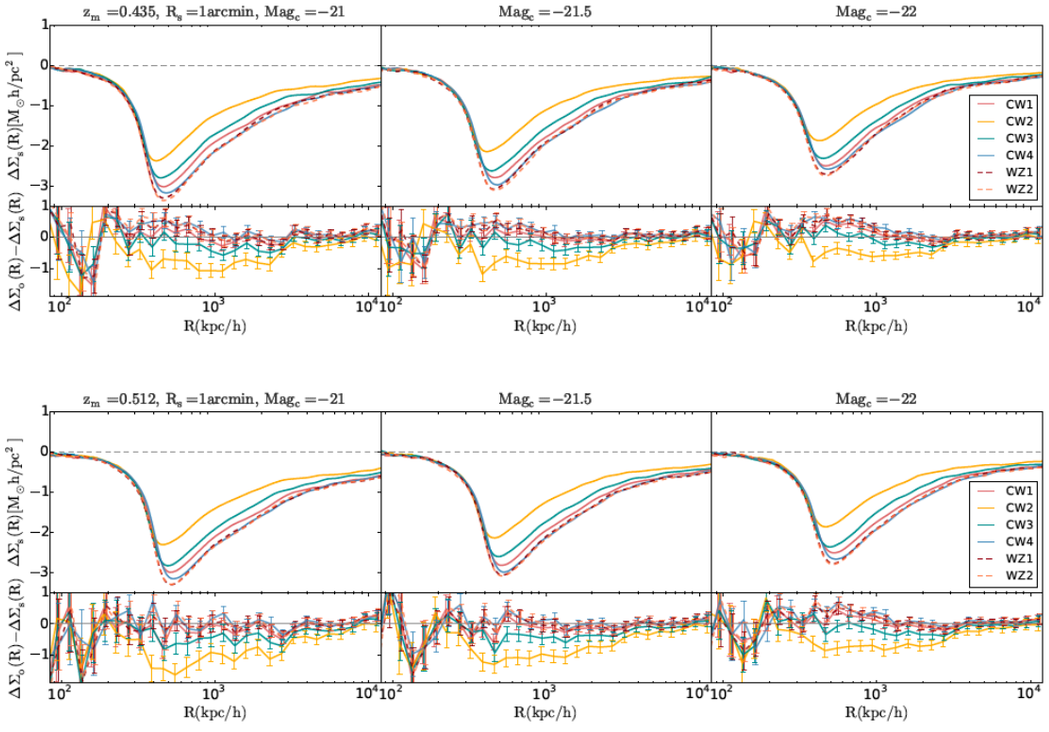

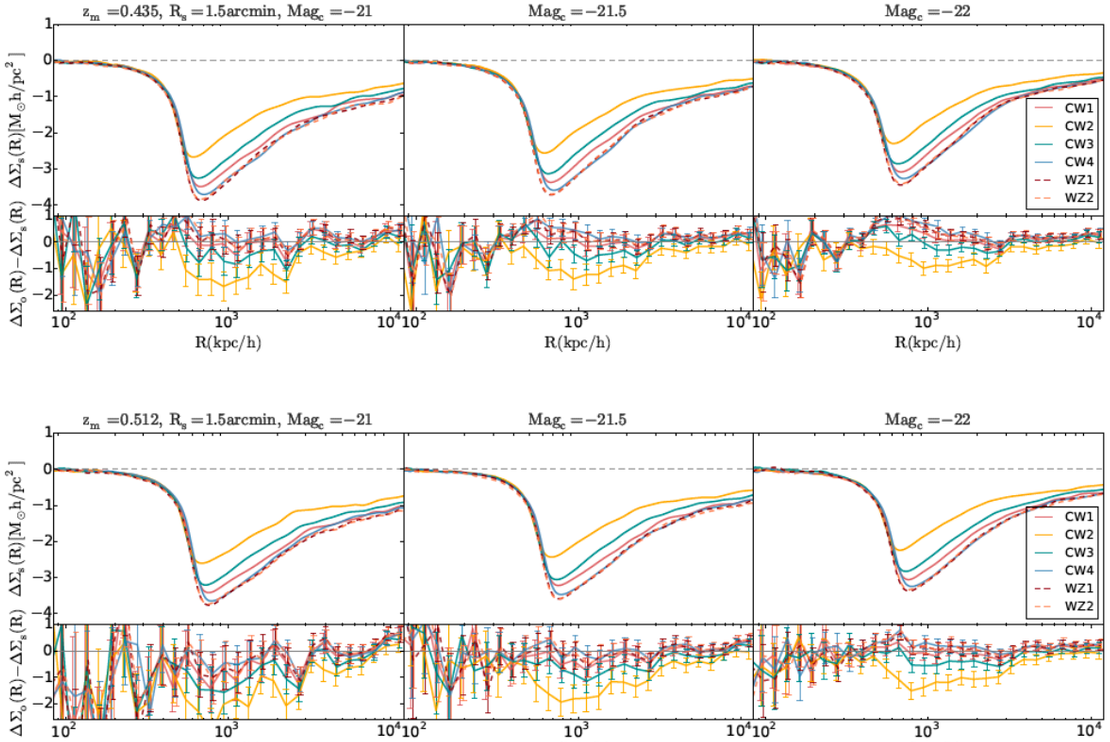

Figure 9. The average excess surface density profile around LDPs that are defined with $R_s = 1$ arcmin and different choices for the magnitude cut and redshift range. The left, middle, and right columns are for $Mag_c = -21, -21.5, -22$ respectively, and the top, middle, and bottom rows for $z_m = 0.35, 0.435, 0.512$. The upper part of each panel shows $\Delta\Sigma_s(R)$ from simulations. The lower part shows the residuals after subtracting $\Delta\Sigma_s(R)$ from $\Delta\Sigma_o(R)$.

(z_m, Mag_c, R_s)
-> Different foreground galaxy
-> Different LDPs

Figure 10. Similar to fig.9, but with $R_s = 1.5$ arcmin.

$$z_m = 0.335, 0.435, 0.512$$

$$Mag_c = -21, -21.5, -22$$

$$R_s = 1, 1.5\ armin$$

Comparing the discrepancy between observational and simulation signal

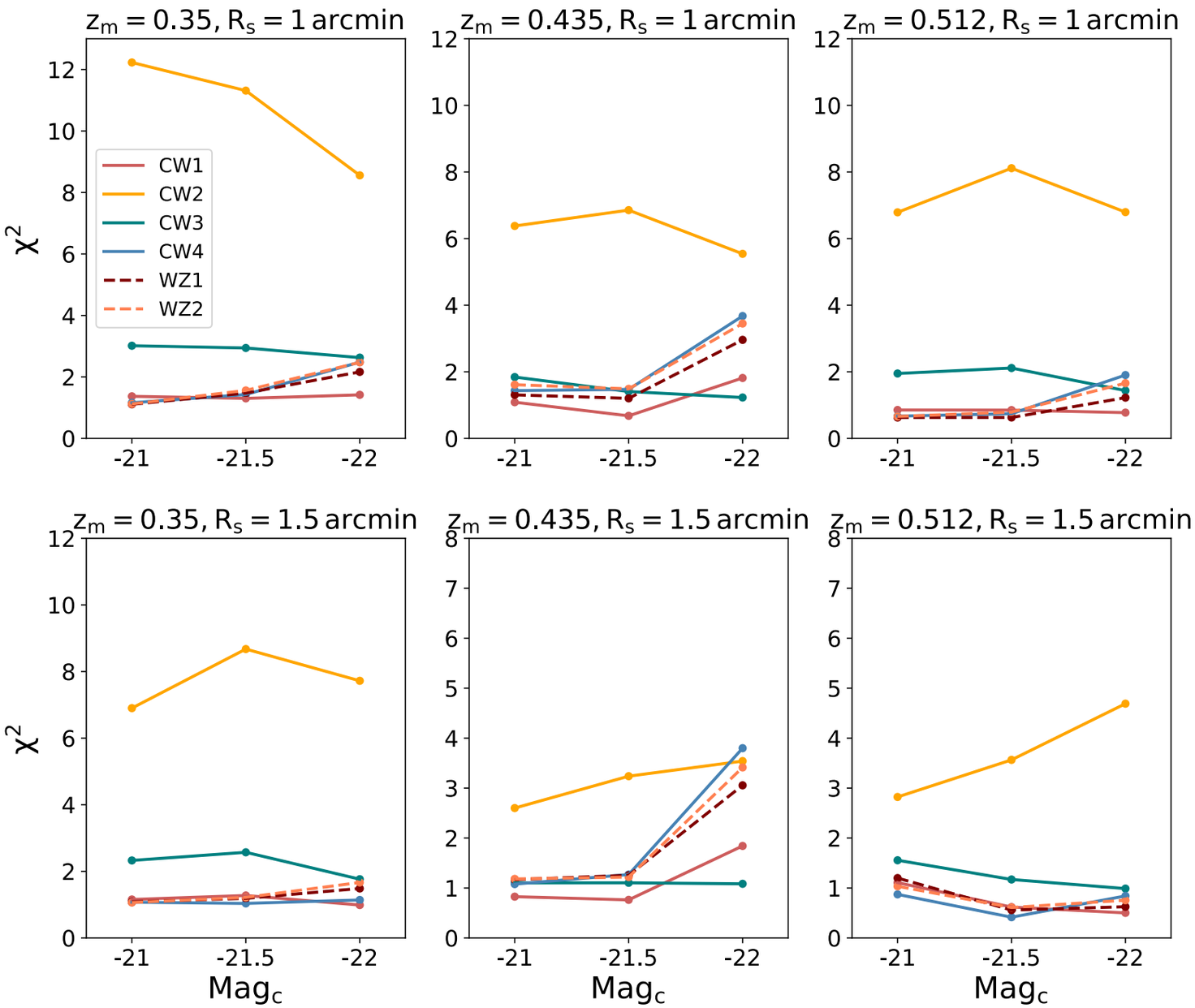

CW1, w=-1
CW2, w=-0.5
CW3, w=-0.8
CW4, w=-1.2
WZ1, w=-1
Wz2, w(z)

$$\chi^2 = \frac{1}{N_{bin}} \sum_{i,j} \delta\Delta\Sigma(\theta_i) C^{-1}_{i,j} \delta\Delta\Sigma(\theta_j), \qquad (9)$$

$$\delta\Delta\Sigma(\theta_i) = \Delta\Sigma_o(\theta_i) - \Delta\Sigma_s(\theta_i).$$

In progress - LDP lensing

1. LDP lensing with the Fourier Quad shear catalogue

Fourier Quad: Zhang et al.(2015)
Fourier Quad pipeline: Zhang et al. (2019)

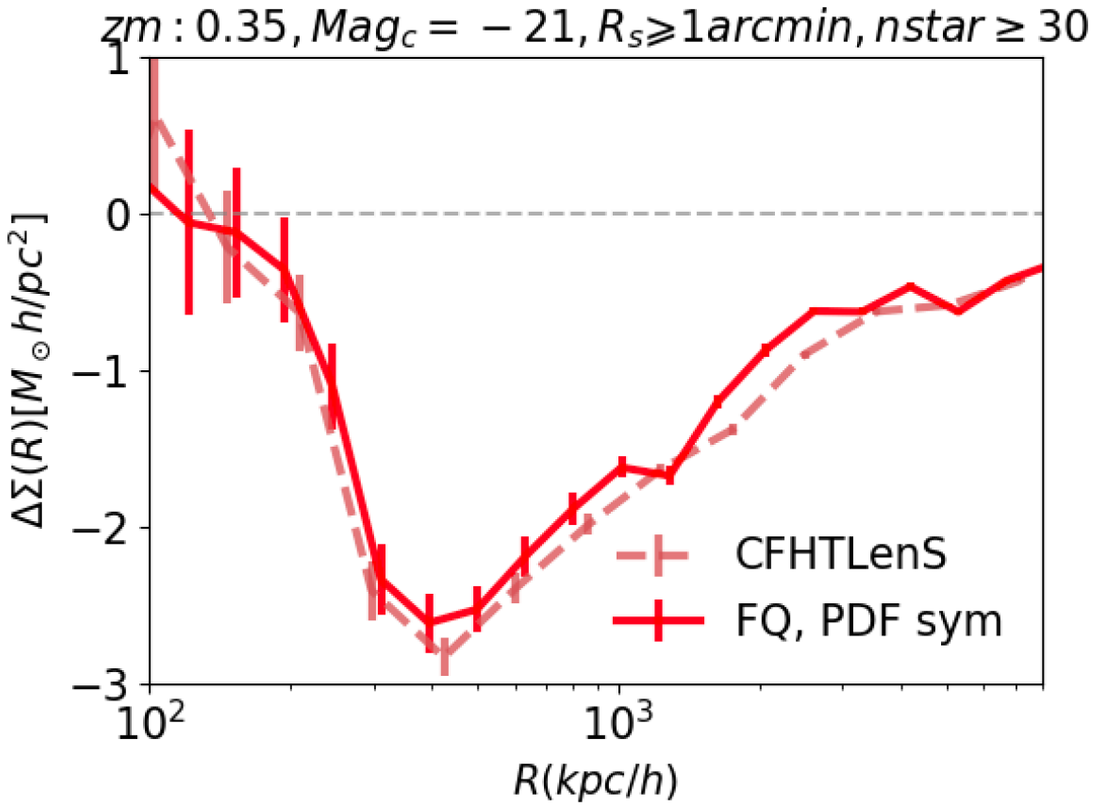

2. LDP Lensing on SDSS

Shear catalogue from Wentao Luo (2017), combining Bernstein & Jarvis (2002, herefater BJ02) & re-Gaussianization Hirata & Seljak (2003)

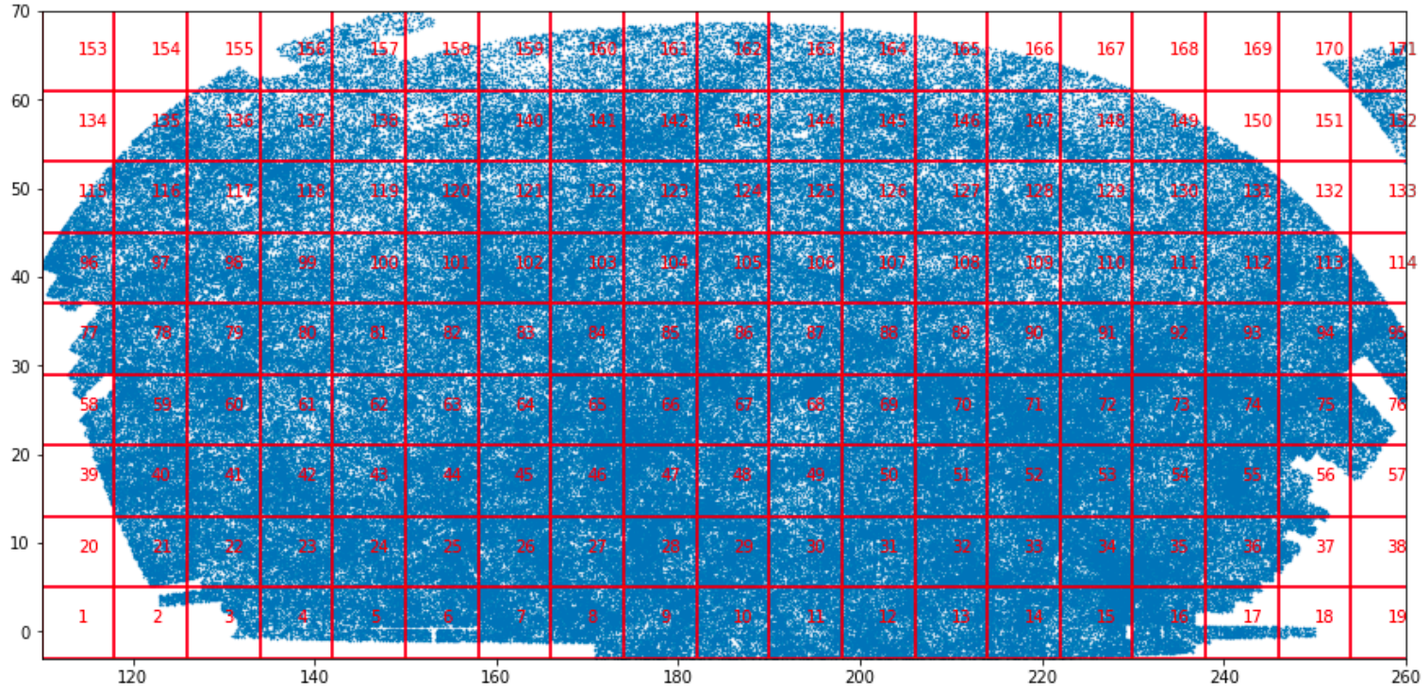

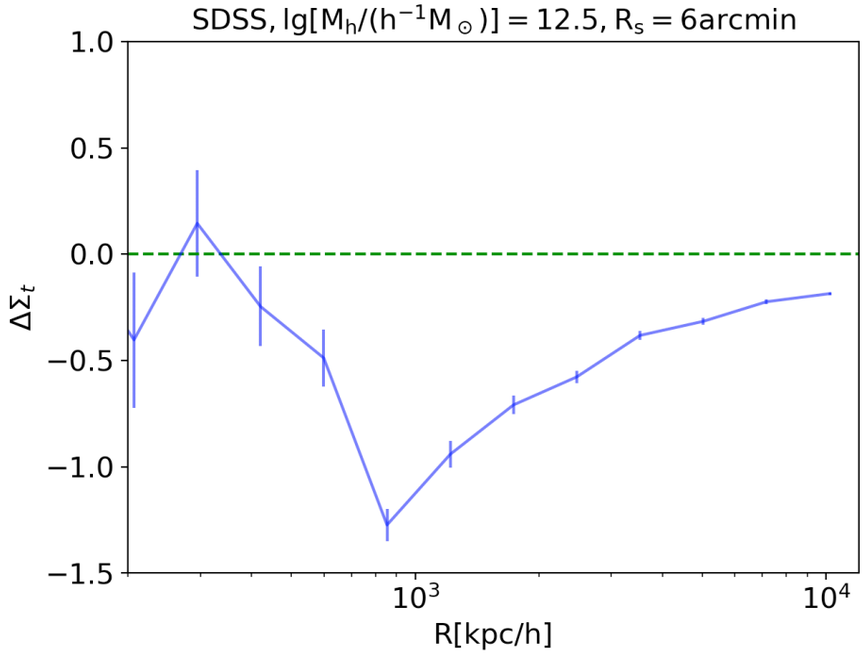

4. Summary

1. We have measured the LDP lensing signals with high SNR with CFHTLenS shear catalogue.
2. With LDP lensing signals, we have made some basic constraints on the w(z).

Future plan:
We are also looking forward to make more accurate constraints on the cosmological parameters with shears measured from larger surveys.

Thank you!